FEM Correlation and Shock Analysis of a VNC MEMS Mirror Segment

E. J. Aguayo*[1], R. Lyon[2], M. Helmbrecht[3], S. Khomusi[1]
[1]The Newton Corporation, Bowie, MD, USA
[2]NASA Goddard Space Flight Center, Greenbelt, MD, USA
[3]Iris AO, Inc., Berkeley, CA, USA
*12603 Safety Turn, Bowie, MD, USA 20715, e.aguayo@thenewtoncorp.com

Abstract: Microelectromechanical systems (MEMS) are becoming more prevalent in today's advanced space technologies. The Visible Nulling Coronagraph (VNC) instrument, being developed at the NASA Goddard Space Flight Center, uses a MEMS Mirror to correct wavefront errors. This MEMS Mirror, the Multiple Mirror Array (MMA), is a key component that will enable the VNC instrument to detect Jupiter and ultimately Earth size exoplanets.

Like other MEMS devices, the MMA faces several challenges associated with spaceflight. Therefore, Finite Element Analysis (FEA) is being used to predict the behavior of a single MMA segment under different spaceflight-related environments. Finite Element Analysis results are used to guide the MMA design and ensure its survival during launch and mission operations. A Finite Element Model (FEM) has been developed of the MMA using COMSOL. This model has been correlated to static loading on test specimens. The correlation was performed in several steps—simple beam models were correlated initially, followed by increasingly complex and higher fidelity models of the MMA mirror segment. Subsequently, the model has been used to predict the dynamic behavior and stresses of the MMA segment in a representative spaceflight mechanical shock environment. The results of the correlation and the stresses associated with a shock event are presented herein.

Keywords: MEMS, Mechanical Shock, Finite Element Modeling, Stress Prediction, Displacement Prediction, Residual Stresses, Deformable Mirror

1. INTRODUCTION

Deformable mirrors are adaptive optics which measure and compensate for optical wavefront aberrations. Typically, deformable mirrors are composed of a multitude of mirror segments. Each one of these mirror segments is individually addressed to correct wavefront errors.

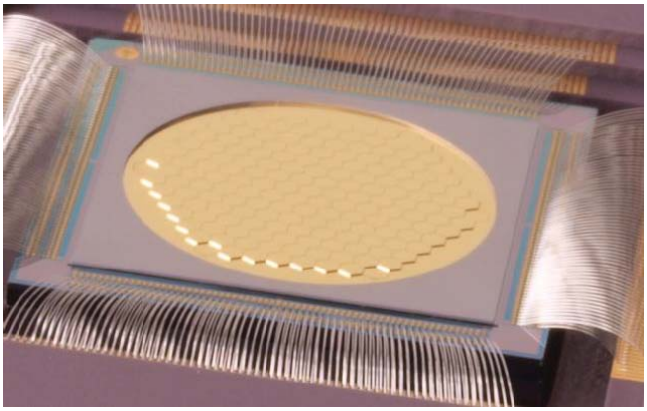

Figure 1. Deformable Mirror System. Deformable Mirror Systems are composed of a multitude of mirror segments.

This type of technology is being developed for use in the Visible Nulling Coronagraph (VNC) instrument at NASA Goddard Space Flight Center. This technology is being called the Multiple Mirror Array (MMA). The MMA will enable the Visible Nulling Coronagraph to detect Jupiter and even Earth sized exoplanets.

Each MMA mirror segment is supported by a Microelectromechanical systems (MEMS) Mirror Segment Platform (MMSP). Since the MMA is being developed for space-based applications it must be capable of surviving launch and other environmental events. Of particular concern are shock events, which have proven challenging on other missions using MEMS devices.

This paper demonstrates the approach taken to create a correlated finite element model (FEM) of the MMSP. This FEM has been used to predict the response of the MMSP to shock events representative of a launch environment. The results obtained for the shock analysis are presented herein.

2. FINITE ELEMENT MODEL CORRELATION

The approach to create a correlated model of the MEMS Mirror segment is to correlate related but simplified parts first. The order and parts that were correlated are: (1) Single layer cantilever beam; (2) Triple layer cantilever beam; and (3) MEMS Mirror Platform.

2.1 Single Layer Cantilever Beam

The first material layer of the MEMS Mirror Platform is thick relative to the second and third material layers. The stress gradient through the thickness of the first material layer, therefore, has a measurable effect on deflections due to residual stresses of the MEMS Mirror Platform. Thus, the first step in creating a correlated model of the MEMS Mirror Platform is to create a correlated FEM of the first material layer. This has been done by creating a single layer cantilever beam, measuring displacements of this item, and correlating the FE model to match the as-measured displacements.

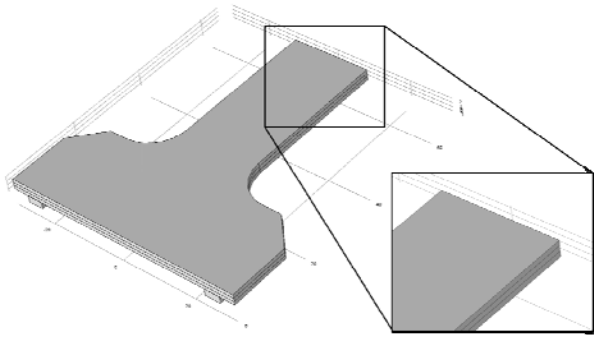

Figure 2. Single Layer Cantilever Beam Geometry for FEM Model. The geometry of the single layer cantilever beam matches the geometry of the test article. The single layer has been divided into three sub-layers, as can be seen in the magnified image.

The Single Layer Cantilever Beam has a similar geometry to that of the MEMS Mirror segment cantilever beams. The main difference is that while the MEMS Mirror Platform's beams are made up of three material layers, this cantilever beam is made of a single material. This material, the first layer material, has a stress gradient through the thickness. Therefore, when the cantilever gets released during the manufacturing process it curls due to the stress gradient. The total displacement of the cantilever beam due to bending has been measured using an interferometer. An FEM of the cantilever beam has been created using COMSOL. The geometry of the FEM matches the geometry of the as-measured component.

The average residual stresses in the cantilever beam have been measured with the wafer curvature method using Stoney's equation[2]:

$$\sigma_f = \frac{E}{6(1-\nu)} \cdot \frac{t_s^2}{t_f} \cdot \left(\frac{1}{R} - \frac{1}{R_0} \right)$$

Where E is Young's modulus, ν is Poisson's ratio, t_s is the thickness of the silicon wafer, t_f is the thickness of the first material layer, R_0 is the initial curvature, and R is the measured radius of curvature.

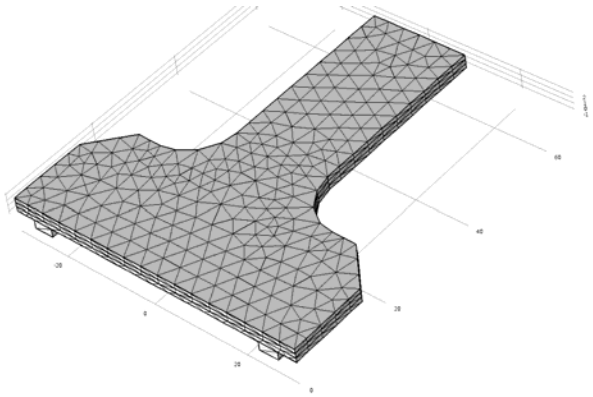

Figure 3. Finite Element Model of the Single Layer Cantilever Beam. Solid elements were used to model the Single Layer Cantilever Beam. Each sub-layer was assigned different residual stresses to approximate the stress gradient through the thickness of the first material layer.

The gradient of the residual stress through the thickness of the first layer has been approximated using the FEM. The first layer was divided into three sub-layers. A linear stress gradient was assumed. The middle sub-layer was set to the average residual stress derived from Stoney's equation. The residual stresses of the top and bottom sub-layers were therefore related by the following equation:

$$\sigma_{average} = \frac{\sigma_{top} + \sigma_{bottom}}{2}$$

(2)

where $\sigma_{average}$ is the average residual stress as derived using Stoney's equation (and the stress of the middle sub-layer), σ_{top} is the residual stress of the top sub-layer, and σ_{bottom} is the residual stress of the bottom sub-layer.

The top and bottom residual stresses were varied to match the deformed shape and total deformation from the as-measured displacements. Figure 4 shows the analytical results and compares them to as-measured data.

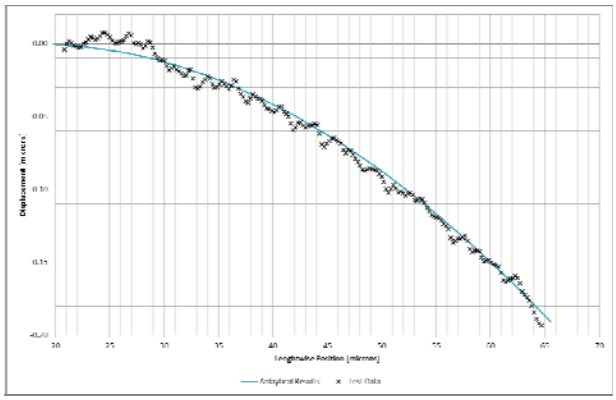

Figure 4. Comparison of Analytical Results and As-Measured Test Data for the Single Layer Cantilever Beam. The residual stresses in the top and bottom sub-layers were tuned to obtain until the analytical displacements matched the as-measured displacements.

The residual stress gradient through the first material layer has been approximated by fine tuning the residual stresses in the top and bottom sub-layers. Figure 2 demonstrates this approximation yields analytical results that correlate closely with as-measured data. The correlated stress values for the first material layer will be used in the subsequent analyses.

2.2 Tri-Layer Cantilever Beam

Most of the displacement of the MEMS Mirror Platform is due to the residual stresses in the three cantilever beams that support the structure. Therefore, a robust correlation of the cantilever beams is necessary.

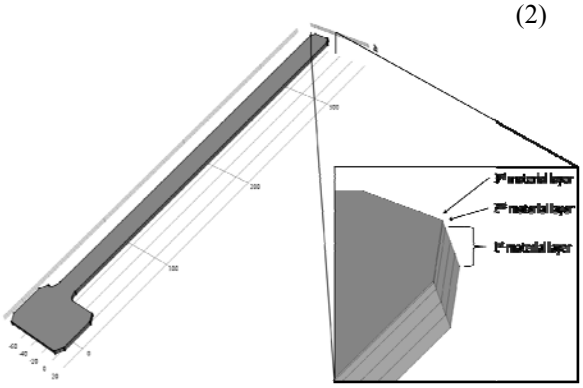

Figure 5. The Tri-Layer Cantilever Beam has three material layers. The bottom layer is composed of three sub-layers. The length of the Tri-Layer Cantilever Beam is the same as the length of the cantilever beams on the MEMS Mirror Platform.

The cantilever beams are composed of three different material layers. Each layer has residual stresses. The average residual stresses in each layer have been determined through Stoney's equation. The gradient of the first material layer has been approximated as previously explained. Any gradients through the thickness of the second and third material layers are negligible because these layers are significantly thinner than the first material layer.

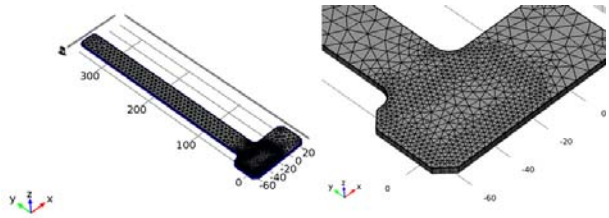

Figure 6. Finite Element model of the Tri-Layer Cantilever Beam. The FEM is composed of solid elements. The first material layer has been assigned the same properties and residual stresses discussed previously in this document. The second and third material layers have been assigned the residual stresses measured using Stoney's equation.

COMSOL has been used to solve the FEM. Since large displacements are expected, the non-linear solver has been used to take into account any geometric non-linearities.

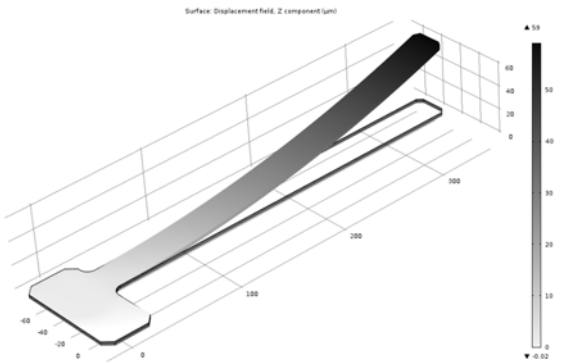

Figure 7. FEM Deformation Results of the Tri-Layer Cantilever Beam. The deformed shape of the Tri-Layer Cantilever Beam is shown above. Displacements and geometry are on a 1:1 scale with respect to each other.

The displacements obtained from the FEA match the as-measured displacements very well. Figure 8 shows the displacements along the length of the Tri-Layer Cantilever Beam. The displacement at the tip of the beam, according to test measurements, is 58 microns. Analysis results indicate the displacement at the tip of the beam is 58.96 micron. The error, 1.7%, is small and demonstrates the FE model is well correlated.

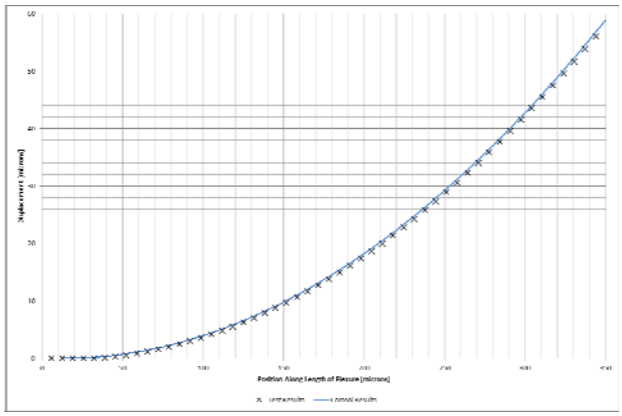

Figure 8. Comparison of Analytical and As-Measured Results for the Tri-Layer Cantilever Beam. Analytical and as-measured results agree very well. The as-measured displacement at the tip is 58 microns, which compares very well with the analytical displacement of 58.96 microns.

2.3 Platform

The material properties and model approach developed during the Single and Tri-Layer Cantilever Beam correlated FEMs were applied to create a model of a complete MEMS Mirror Platform. An FE model was created of the MMSP. The FEM geometry reflects the geometry of the unit used to take displacement measurements.

The FEM was used to predict the displacement of the platform due to residual stresses in the different material layers. Each material layer has the same material properties as those used in the correlated single and tri-layer cantilever beam models. The results of the FE analysis predict displacements very similar to those measured on the test item.

Table 1 shows the vertical displacement of the Platform at three specific points. Analytical results are very close to the as-measured results. The largest difference between analytical and as-measured results, for the three points shown, is 1.56 microns. Relative to the As-Measured displacement of 25.87 microns, this is a 6% error, which is acceptable for future analysis.

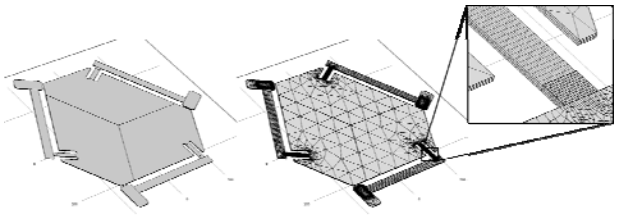

Figure 9. Geometry and FEM of the MEMS Mirror Segment Platform. The FEM reflects the geometry of the unit used to take displacement measurements. Additional mesh detail was added to regions of high stress.

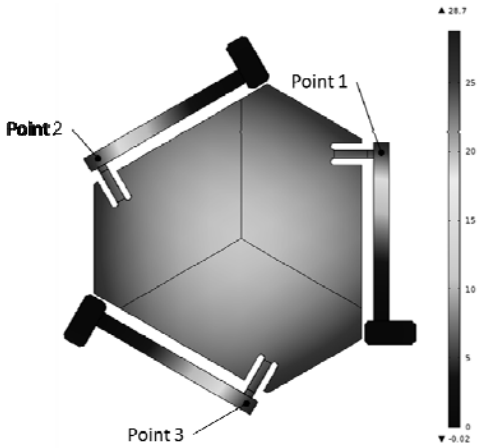

Figure 10. Analytical displacements of the MEMS Mirror Segment Platform. Analytical displacements of the platform agree well with the as-measured displacements. Points for comparison between analytical and as-measured results are shown.

In an effort to simplify the geometry for further, more computer intesive analyses, the anchors of the catilever beams were removed. The displacements of the platform were then compared between these two models.

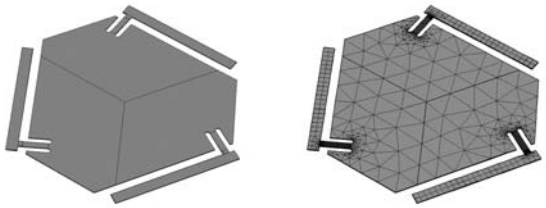

Figure 11. Geometry and FEM of the MEMS Mirror Segment Platform without Anchors. This simplified model of the MMSP was evaluated and it was determined it can be used for further analyses.

Displacements at three discrete points, as those shown in Figure 10 and Table 1, were evaluated for the models with and without anchors. These results are presented in Table 2. The results from both models are very close to the results obtained from the more complex model which includes anchors. The largest error is 2.76 micron, or about 10.6%. This error is acceptable to reduce computation time for further analyses.

3. SHOCK ANALYSIS

Often, one of the main concerns with MEMS devices is their ability to survive launch. Shock is of particular concern for the MEMS Deformable Mirror. Therefore, a shock analysis has been performed to evaluate the robustness of the design. Future tests will be performed and results from these tests will be correlated with the analytical results presented herein.

The Delta IV Rocket can have significant shock levels[1]. These shock levels are being used to validate the design of the MEMS Deformable Mirrors. These levels are presented in Table 3 and Figure 12. These levels are used in this analysis to get an initial understanding of the behavior of the MEMS Deformable Mirror segment.

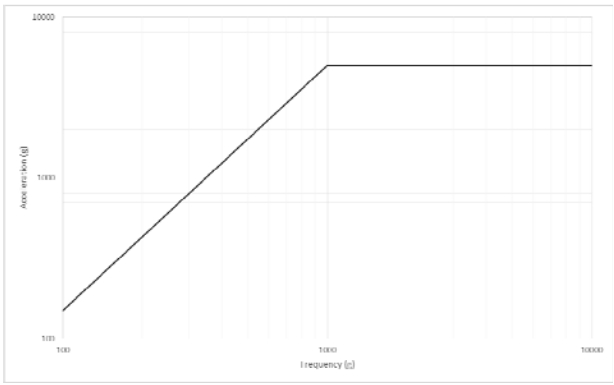

Figure 12. Shock response spectrum of high-level shock tests for MEMS Deformable Mirrors.

A time history has been synthesized based on the shock response spectrum (SRS) presented in Table 3 and Figure 12. The time history is composed of sine wavelets. The time history synthesized is presented in Figure 13.

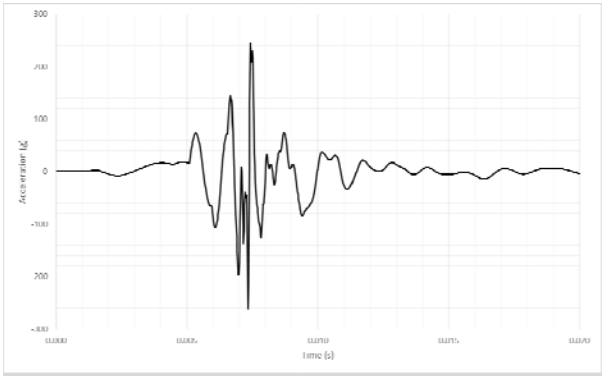

Figure 13. Synthesized time history to match the prescribed SRS. A time history has been synthesized using wavelets to match the required SRS.

The synthesized time history has been applied to the FE model of the MMSP. It has been applied in the out-of-plane direction, which will create the greatest displacements and highest stresses. The initial condition of the MMSP includes the residual stresses, which create the initial displacements and stress state delineated in the correlation section of this document. The residual stresses are applied throughout the acceleration loading as well.

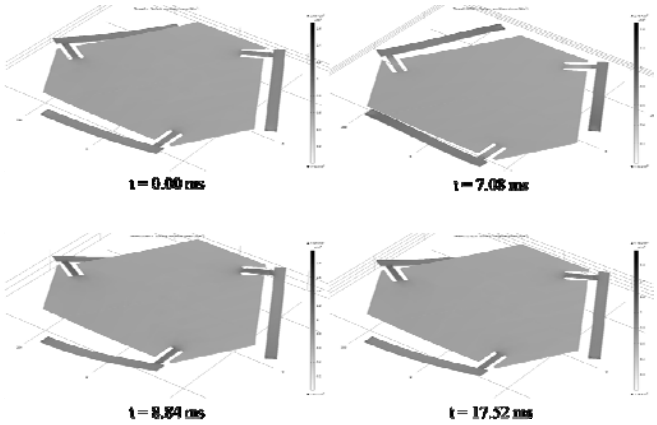

Figure 14. Deformations of the MMSP due to residual stresses and shock input. The platform deforms and displaces due both to the input load and the residual stresses in the different material layers. Deformations and the geometry are on a 1:1 scale relative to each other.

Displacement history at one of the torsion flexures is shown in Figure 15 and provides a good indication of the response of the MMSP to the shock load. Notice that the analysis is predicting negative displacements. This is an indication that the MMSP is likely to impact the substrate below. Further analysis and testing will be required to establish both the validity of the prediction and the possible ramifications of contact events.

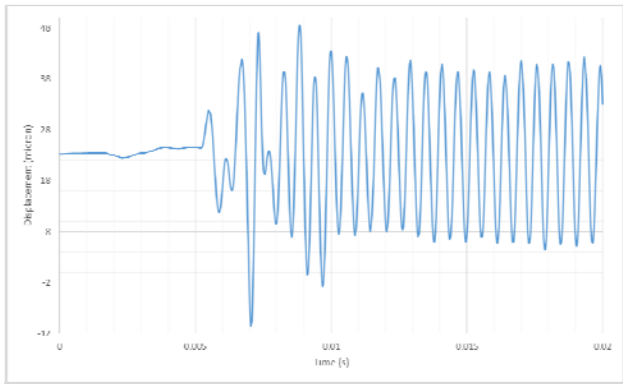

Figure 15. Displacement of the MMSP due to shock.

Similarly, the maximum principal stresses on the torsion flexures are tracked as a function of time during the shock event. The maximum stress predicted is 1957 MPa, which occurs at 8.84 ms. The allowable for the material at locations of high stress concentrations, as occurs in the MMSP, is of approximately 7.9 GPa. Thus, the analysis predicts the MMSP should survive a shock event of this magnitude. However, this analysis does not take into consideration the effects of likely impacts between the MMSP and the underlying substrate. These impacts are being predicted based on the negative displacements of the MMSP.

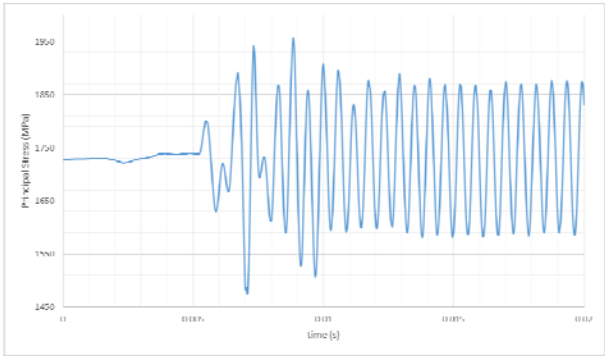

Figure 16. Principal stresses in the MMSP during a shock event. Principal stresses in the MMSP reach levels as high as 1.96 GPa, which are within the expected allowable of 7.9 GPa for this material.

4. CONCLUSIONS AND FUTURE WORK

Steps were taken to create a correlated FE model of the MMSP. These steps involved creating correlated models of subcomponents of the overall MMSP. Thus, the completed model is based on simpler, easy to correlate models. The completed model of the MMSP has been used to predict displacements and stresses due to a shock input. While stress predictions are benign, displacements indicate the MMSP will likely impact the substrate below it. This analysis does not account for impact or the stress effects the impact might have on the MMSP.

Future analysis is still needed to refine these findings. For example, different damping values should be studied—a relatively low value of the quality factor (Q = 30) was chosen for this analysis due to the expected significant effect of air damping on a MEMS device. However, it is possible for this device to experience shock events in a rarified air environment or even in vaccuum, since it is intended to be used for space applications.

5. REFERENCES

[1] The Boeing Company, "The Delta IV Payload Planners Guide," MDC 99H0065, (1999).

[2] Stoney G. "The tension of metallic films deposited by electrolysis," Proc. Royal Soc. London, A82 (1909) 172-175.

Frequency (Hz)	Q Level (10) Three Mutually Perpendicular Axes
	High-level
100	150 g
100–1,000	+9.2 dB/oct
1,000–10,000	5,000 g

6. APPENDIX

Table 1. Comparison of as-measured and analytical displacements of the MEMS Mirror Segment Platform at three discrete points. As-measured and analytical displacements of the platform agree well.

	Location [um]		**Displacement [um]**	
Point ID	**X**	**y**	**As-Measured**	**Analysis**
1	261	158	25.87	24.31
2	-266	147	24.95	24.15
3	5.9	-305	26.05	24.83

Table 2. Comparison of analytical displacements of the MEMS Mirror Segment Platform at three discrete points. An MMSP with anchors model was compared to one without anchors. The results between the models demonstrates errors in displacement are small when the anchors are omitted from the model.

	Location [um]		**Displacement [um]**	
Point ID	**x**	**y**	**With Anchors**	**No Anchors**
1	261	158	24.31	23.17
2	-266	147	24.15	23.18
3	5.9	-305	24.83	23.29

Table 3. Shock response spectrum of high-level shock tests for MEMS Deformable Mirrors. Lawson et al established these shock levels as the worst case scenario shock environment for MEMS Deformable Mirrors on an Exoplanet Mission.